

Ab Initio Calculations on Uracil–Water

Tanja van Mourik,* Sarah L. Price, and David C. Clary

University College London, Centre for Theoretical and Computational Chemistry, Department of Chemistry, 20 Gordon St., London WC1H 0AJ, U.K.

Received: August 11, 1998; In Final Form: November 13, 1998

The potential energy surface for the interaction of uracil with one water molecule is investigated using ab initio techniques. The structures of four cyclic minima, as well as two transition-state structures, have been determined using second-order Møller–Plesset perturbation theory (MP2) and the interaction-optimized DZPi basis set. At the optimized geometries, the counterpoise-corrected interaction energies have also been computed with a slightly larger basis set containing bond functions, labeled ESPB. The MP2/ESPB calculations predict D_e for the four uracil–water minima to be -40.0 , -31.8 , -33.5 , and -26.6 kJ/mol. The barrier height between the global minimum and the adjoining local minimum (with $D_e = -31.8$ kJ/mol) is found to be as much as 23 kJ/mol, while the barrier height between the two most stable local minima ($D_e = -33.5$ and -31.8 kJ/mol) is only 10 kJ/mol. For the global minimum we also investigated the effect of basis set superposition error (BSSE) on the two hydrogen bond distances, as well as the effect of freezing the monomer geometries during optimization. It is found that BSSE decreases the hydrogen bond lengths by about 0.1 Å, while freezing the intramolecular geometries reduces the uracil–water interaction energy by less than 2 kJ/mol.

1. Introduction

The hydration of biomolecules is vitally important in molecular biology, since numerous biological processes involve a ligand binding to a nucleic acid or protein and thereby displacing the water of hydration. Thus, accurate force fields for the interactions of nucleic acid or protein fragments with water are required for realistic simulations of biochemical processes. Unfortunately, a biomolecule–water potential energy surface cannot be constructed from accurate ab initio calculations, even with the recent growth in computer power, because too many points are required. For example, Mok et al.¹ needed 20 480 numerical quadrature points to characterize the six-dimensional intermolecular potential for the water dimer using density functional theory. Clearly, the construction of such a potential energy surface for larger (biomolecular) systems, using more elaborate ab initio techniques, is currently not feasible. However, ab initio studies on the key geometries on the potential energy surface can provide accurate energies at these points, as well as providing valuable insight into the details of the interaction.

In the present study we investigate several stationary points on the uracil–water potential energy surface using ab initio methods. Uracil is a nucleic acid base occurring in RNA (ribonucleic acid). The uracil molecule contains a row of alternating C=O and N–H groups, which provide a range of possible hydrogen-bonded arrangements for the water molecule. The structures investigated in this work are depicted in Figure 1. In all of these the water molecule is bonded to uracil via two hydrogen bonds (an OH···O and an NH···O bond in complexes 1–3 and an OH···O and CH···O bond in complex 4). A scan of the uracil–water potential energy surface, using the ORIENT² program and a model potential consisting of a hard-sphere repulsion for each non-hydrogen atom and an accurate description of the electrostatic contribution, calculated from the multipoles obtained by a distributed multipole (DMA^{3,4}) model

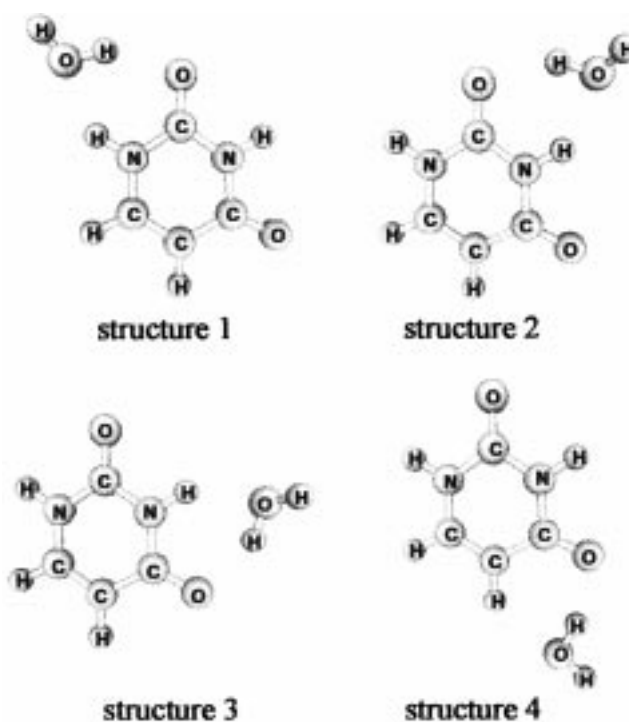


Figure 1. Four hydrogen-bonded uracil–water complexes considered in this work. The water molecule is bonded to uracil via two hydrogen bonds (an OH···O and an NH···O bond in complexes 1–3 and an OH···O and CH···O bond in complex 4). The water OH bond that is involved in forming the hydrogen bonds is situated in the plane of the uracil molecule. The free water H-atom is pointing out of the plane in complexes 1–3, while in complex 4 the water monomer is entirely in the plane of the uracil molecule.

of the MP2/6-311G** monomer wave functions, yielded the same (qualitatively equivalent) four minimum-energy structures as depicted in Figure 1. Since the orientation dependence of the electrostatic energy closely resembles that of the total

* Corresponding author. E-mail address: t.vanmourik@ucl.ac.uk.

energy,⁵ we expect that this survey has yielded all major minima on the potential energy surface.

Recent diffusion Monte Carlo (DMC) studies^{6–10} have shown that the zero-point vibrational motion in hydrated clusters has a wide amplitude and may cause significant reorientation of the hydrogen bonds. These vibrational motions may allow the water molecules to move over different hydration sites in these clusters. The uracil–water minima lie on adjacent positions around the ring, which suggest that the barriers between the minima could be relatively small, resulting in motion between the minima. Thus, our study of the uracil–water interaction included calculations on the transition states connecting the three lowest minima, since these barriers will play a major role in determining the dynamics of the hydration of uracil.

In the past, ab initio calculations on biomolecular systems have been mainly performed at the Hartree–Fock SCF (self-consistent field) level of theory, while the BSSE (basis set superposition error) is generally left uncorrected. In light of the severe approximations involved in such studies, these cannot be deemed very reliable. There have been a few studies on the uracil–water complex that include electron correlation,^{11–13} but none of these studied all the minima or any transition states.

The first correlated calculations on the uracil–water system were performed by Rybak et al.¹¹ They computed the uracil–water interaction energy at two planar configurations, both obtained from no-CP (no-counterpoise) SCF calculations,^{14,15} using many-body symmetry-adapted perturbation theory (SAPT) in combination with supermolecular calculations and a minimal basis set augmented with a single polarization function on each atom. The structures investigated were similar to geometry **1** in Figure 1, which was established to be the minimum-energy configuration in the no-CP SCF calculations.

For a study of dipole-bound electron attachment to uracil–water complexes, Smets et al.¹² performed MP2/6-31++G** calculations on three uracil–water geometries, which were first optimized at the SCF/6-31+G* level of theory. They reported that complex **1** was the most stable structure followed by complex **3** and then **2**. Smets et al.¹³ also studied electron attachment to the uracil–(H₂O)₃ complex, in which the water sites 2 and 3 cannot be populated simultaneously, since formation of two hydrogen bonds by a single hydrogen atom is not possible. To allow each of the three water molecules to form two hydrogen bonds with uracil, the third water molecule has to occupy site 4, thus showing structure **4** (see Figure 1) as a plausible local minimum on the uracil–water potential energy surface.

Potential energy surfaces of molecular complexes may be distorted if the effect of BSSE on the computed geometries is neglected. Optimizing the structures of weakly bound complexes without correcting for BSSE generally yields too short intermolecular distances.^{16,17} For (HF)₂ for example, which has a binding energy of 19 kJ/mol (about half the interaction energy of the global uracil–water minimum), optimization of the geometry without the counterpoise correction leads to an F...F distance that is too short by 0.06 Å at the MP2/aug-cc-pVDZ level of theory.¹⁸ Likewise, at the same level of theory the O...O distance in (H₂O)₂ is too short by the same amount (i.e., 0.06 Å) if BSSE is ignored during the optimization.¹⁹ These shortenings are highly basis-set-dependent.^{17,19,21} To assess the effect of BSSE on the uracil–water geometry, employing the basis sets used in the present study, we will investigate the influence of BSSE on the two hydrogen bond distances of the global uracil–water minimum.

The paper is organized as follows. In section 2, we shortly describe the theory related to the computation of counterpoise-corrected potential energy surfaces followed by a discussion of the basis sets used in this study, whereupon the methodology employed to locate the stationary points is presented. Section 3 presents the results of the ab initio calculations. We first compare the total energies and dipole moments of uracil, computed with several different basis sets, since the charge distribution in the uracil monomer may affect the structure of the uracil–water complex. Second, the results for the global minimum are presented. For this minimum we also investigate the effect of BSSE on the computed hydrogen bond distances and take a closer look at the effect of freezing the monomer geometries in the optimizations. Next, the optimized structures and interaction energies of all four uracil–water minima, as well as the transition states between structures **1** and **2** and structures **2** and **3** are presented. Section 4 summarizes the results.

2. Methodology

2.1. Basis Sets. To optimize the structure of a single stationary point on the uracil–water potential energy surface, generally around 20–30 energy evaluations are required. We therefore need to employ a basis set that is sufficiently compact to allow a reasonably quick evaluation of the uracil–water energy. One basis set that fulfills this requirement is the singly polarized double- ζ (DZP) basis set, with which one optimization step at the MP2 (second-order Møller–Plesset) level of theory takes about 2 h of computation time on an SGI Power Challenge (with the Gaussian 94 program package²¹). However, interaction energies using DZP sets are known to be highly dependent on the exponents of the polarization functions employed.²² Generally, the exponents are obtained by minimization of the total energy at the MP2 level, but it was shown²³ that such energy-optimized basis sets are not the optimal choice for calculations on molecular complexes involving polar molecules. This has led to the development of an *interaction-optimized* DZP basis set for (H₂O)₂, for which the exponents were chosen for effective calculation of the interaction energy by considering various energy components.²² In the present study, we have used a slightly different interaction-optimized DZP basis set, labeled DZPi,²³ obtained in a manner similar to that of the sets reported in ref 22. DZPi consists of a double- ζ (DZ) set, which is (9s5p) contracted to [4s2p] on C, N, and O, and (4s) contracted to [2s] on H, augmented with a single set of polarization functions (P) on each atom. We have used Dunning's DZ set^{24,25} in this work. The exponents of the polarization functions of DZPi were obtained by optimizing the interaction energy contributions of selected small van der Waals complexes. The optimized exponents are 0.387 for the p-polarization function on H and 0.256, 0.32, and 0.40 for the d-polarization functions on C, N, and O, respectively.²³

Although the DZPi basis set yields much better interaction energies than energy-optimized basis sets of comparable size, it was concluded²³ that for high precision larger basis sets containing more polarization functions and a set of bond functions must be employed. Calculations on uracil–water with such basis sets will, however, be prohibitively large. As a compromise, we have performed single-point calculations with a basis set that is only slightly larger than DZPi. This basis, ESPB,²⁰ is derived from DZPi by replacing the (9s) \rightarrow [4s] part of C, N, and O by an ES (extended s) set, which is (10s) contracted to [5s]. The additional s function is taken from the compact isotropic (10s6p) \rightarrow [5s3p] EZ (extended zeta) set^{23,26} that contains, compared to DZ, an additional s and p function,

which are chosen not to be energy-optimized but to resemble the more diffuse exponents of large basis sets such as (13s8p). In addition, ESPB contains a set of (s,p) bond functions (B) with exponent 0.60 placed at the midpoint of the donor(H)⋯acceptor(O) bond. Because the uracil–water minimum-energy structures investigated in this work contain two hydrogen bonds, two sets of bond functions have been used. For (H₂O)₂ ESPB yields SCF and MP2 results of comparable quality as the much larger doubly polarized sets.²⁰ Since the geometry and energy of the water dimer are adequately described at the MP2 level of theory, we expect to obtain reliable energies and structures for uracil–water at the MP2/ESPB level of theory.

To optimize the uracil monomer geometry, the augmented correlation consistent double- ζ (aug-cc-pVDZ) of Dunning²⁷ has been used, which is a (10s5p2d) contracted to [4s3p2d] set on C, N, and O and (5s2p) \rightarrow [3s2p] on H and is therefore, in the terminology from above, a doubly polarized DZ set. The correlation consistent basis sets have been optimized for correlated calculations on the valence electrons of atoms and molecules. Additionally, we optimized the uracil molecule with the triple split valence basis set 6-311G*,²⁸ containing one set of d-polarization functions on non-hydrogen atoms, and with the split valence 6-31+G* basis set,^{29–31} containing a set of diffuse s and p functions as well as a set of d-polarization functions on non-hydrogen atoms. Since uracil is essentially planar in the gas phase,³² the optimizations of the uracil geometry were carried out in C_s symmetry.

2.2. Computation of the Interaction Energy. The geometries of four cyclic uracil–water minima and two transition states connecting the three most stable minima were optimized at the MP2 level of theory, using the DZPi basis set. For each optimized structure, we subsequently performed a single-point calculation with the ESPB basis set. Throughout, only the valence electrons were correlated.

The uracil–water interaction energy is computed as the difference of the energy of the complex and the sum of the energies of the separated monomers. The counterpoise procedure of Boys and Bernardi³³ is applied to circumvent the basis set superposition error (BSSE). The counterpoise-corrected interaction energy at a particular uracil–water geometry (\mathbf{R} , \mathbf{r}_u , \mathbf{r}_w) follows from

$$\Delta E^{\text{CP}}(\mathbf{R}, \mathbf{r}_u, \mathbf{r}_w) = E_{\text{uw}}^{\text{dcbs}}(\mathbf{R}, \mathbf{r}_u, \mathbf{r}_w) - E_{\text{u}}^{\text{dcbs}}(\mathbf{R}, \mathbf{r}_u, \mathbf{r}_w) - E_{\text{w}}^{\text{dcbs}}(\mathbf{R}, \mathbf{r}_u, \mathbf{r}_w) + \Delta U_{\text{u}}^{\text{def}}(\mathbf{r}_u) + \Delta U_{\text{w}}^{\text{def}}(\mathbf{r}_w) \quad (1)$$

where \mathbf{R} denotes the intermolecular geometrical parameters and \mathbf{r}_u and \mathbf{r}_w are the intramolecular geometries of the uracil and water fragment, respectively. (The subscripts u, w, and uw denote uracil, water, and uracil–water, respectively.) The superscript dcbs, which stands for “dimer-centered basis set”, indicates that the uracil and water energies are computed using the complete dimer basis set. The last two terms in eq 1 represent the deformation energies of uracil and water. These describe the energy required to bring a free uracil or water molecule to a particular geometry \mathbf{r}_u or \mathbf{r}_w . The deformation energy of uracil, for example, is computed as the difference of the energy of the uracil molecule fixed at the geometry it has in the complex and the energy of a free uracil at its equilibrium geometry \mathbf{r}_e :

$$\Delta U_{\text{u}}^{\text{def}} = E_{\text{u}}^{\text{mcbs}}(\mathbf{r}_u) - E_{\text{u}}^{\text{mcbs}}(\mathbf{r}_e) \quad (2)$$

$\Delta U_{\text{u}}^{\text{def}}$ is computed in the monomer basis set (mcbs = monomer-centered basis set) at the same level of theory as used for the other terms. However, in most calculations the uracil molecule

was kept fixed at the geometry optimized with the aug-cc-pVDZ basis set, while the water molecule was kept fixed at the geometry optimized by Frisch et al.³⁴ at the MP2/6-311++G-(2d,2p) level of theory (OH distance is 0.9571 Å; HOH angle is 104.34°). In optimizations in which the intramolecular geometries are kept frozen, ΔU^{def} has a constant value at each point on the potential energy surface and thus may be assumed to be zero.

A counterpoise-corrected geometry optimization would require minimization of eq 1, instead of minimization of just E_{uw} . However, automated optimization algorithms based on eq 1 have not been implemented yet, and therefore, fully counterpoise-corrected geometry optimizations of uracil–water will be a formidable, if not impossible, task. In the present paper the geometry optimizations of the uracil–water structures were performed using standard analytical derivative techniques, which operate on the uncorrected total energy E_{uw} , and thus, no BSSE corrections were applied during the optimizations. At the resulting optimized geometry, the interaction energy was computed using eq 1. The interaction energy at the equilibrium geometry of uracil–water will be denoted subsequently as D_e .

This procedure only removes BSSE artifacts in the interaction energy at the “uncorrected” geometry, i.e., optimized without application of the counterpoise method, and this geometry may therefore be distorted compared to the counterpoise-corrected geometry. To estimate the error inherent to this approach, we have investigated the effect of BSSE on the computed O⋯H_w and O_w⋯H hydrogen bond distances (the w subscript indicates the atom belongs to the water moiety) of the global minimum in the following way. Starting from the uracil–water geometry obtained from the uncorrected optimizations as described above, in which the monomer geometries were kept fixed at the aug-cc-pVDZ (uracil) and 6-311++G(2d,2p) (water) optimized geometries, the water molecule was moved along the R(O⋯H_w) direction. The MP2/DZPi interaction energy was computed at four additional values of R(O⋯H_w), obtained by increasing this distance with increments of 0.067 Å. A polynomial of third degree in R(O⋯H_w) was fitted through the resulting interaction energies. Next, the interaction energy was computed at three different values of the O_w⋯H bond distance, starting from the geometry with the optimized O⋯H_w distance, by moving the water molecule along R(O_w⋯H) with increments of 0.033 Å. A polynomial of second degree in R(O_w⋯H) was fitted through the resulting interaction energies.

2.3. Electronic Structure Codes and Computers. The calculations were performed with Gaussian 94²¹ and Molpro96³⁵ on SGI Power Challenges at the Royal Institution and the University College London. Unless stated otherwise, Gaussian orbitals with spherical harmonics for the angular parts were employed. The uracil dipole moment was evaluated at the MP2 level of theory with NWChem,³⁶ employing Cartesian basis functions, on a 300 MHz Pentium II PC running Linux. NWChem computes the MP2 dipole moments from the linear response density matrix.³⁷

3. Results

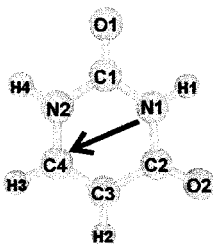
3.1. Calculated Energetics and Dipole Moments of Uracil.

Table 1 shows a comparison of the computed bond distances and bond angles of uracil (the numbering of the atoms in the uracil molecule is depicted in Figure 2), computed with MP2 and several different basis sets. Since DZPi is an interaction-optimized basis set, it is not optimal for optimizing monomer geometries. Energy-optimized basis sets of similar (or larger) size are expected to give more reliable uracil geometries. As shown in Table 1, the energy-optimized basis sets aug-cc-pVDZ

TABLE 1: Geometrical Parameters of Uracil Obtained from MP2 Calculations

	MP2/ DZPi	MP2/ aug-cc-pVDZ	MP2/ 6311G*	MP2/ D95V** ^a	exptl ^b
Bond Length/Å					
C1–N1	1.413	1.389	1.385	1.386	1.377
N1–C2	1.436	1.413	1.408	1.409	1.371
C2–C3	1.483	1.463	1.460	1.461	1.430
C3–C4	1.379	1.364	1.353	1.359	1.340
C4–N2	1.404	1.381	1.375	1.380	1.359
N2–C1	1.417	1.394	1.390	1.391	1.371
C1–O1	1.258	1.228	1.214	1.226	1.215
C2–O2	1.262	1.231	1.218	1.230	1.245
N1–H1	1.031	1.018	1.012	1.014	0.877
C3–H2	1.096	1.089	1.082	1.080	0.931
C4–H3	1.099	1.092	1.085	1.083	0.957
N2–H4	1.025	1.014	1.008	1.010	0.836
Bond Angle/deg					
C1–N1–C2	128.33	128.40	128.81	128.68	126.7
N1–C2–C3	113.59	113.57	113.15	113.26	115.5
C2–C3–C4	119.85	119.65	119.83	119.80	118.9
C3–C4–N2	121.81	121.75	121.88	121.76	122.3
C4–N2–C1	123.61	123.67	123.75	123.68	122.7
N2–C1–N1	112.80	112.96	112.58	112.82	114
O1–C1–N1	124.12	124.07	124.32	124.12	122.3
C1–N1–H1	115.46	115.39	115.28	115.25	117.8
C2–N1–H1	116.21	116.21	115.91	116.07	115.5
N1–C2–O2	120.17	120.31	120.70	120.49	119.2
C3–C2–O2	126.23	126.12	126.15	126.25	125.3
C2–C3–H2	118.54	118.81	118.46	118.67	118.1
C4–C3–H2	121.60	121.54	121.70	121.53	123
C3–C4–H3	122.65	122.65	122.59	122.59	123.2
N2–C4–H3	115.54	115.60	115.53	115.65	114.5
C4–N2–H4	121.13	121.26	121.13	121.22	122.12
C1–N2–H4	115.26	115.07	115.11	115.10	115.1
N2–C1–O1	123.08	122.97	123.11	123.07	123.7

^a Reference 52. ^b X-ray data (ref 38). Data containing H-atoms determined through the experimental accuracy limit.

**Figure 2.** Numbering of atoms and direction of the dipole moment of uracil.

(which we used to optimize the uracil geometry used in the frozen-monomer calculations presented in the next section), 6-311G*, and D95V** yield bond distances that are shorter than the corresponding DZPi results by 0.01–0.05 Å, while the angles differ from the DZPi values by up to 0.5°. The bond distances obtained with aug-cc-pVDZ, 6-311G*, and D95V** differ by only 0.001–0.01 Å, while the bond angles differ by up to 0.4°. Also listed in Table 1 are the experimental geometrical parameters obtained by X-ray crystallography,³⁸ even though these are not directly comparable to the gas-phase data (the molecular packing in the crystal imposes constraints on the geometry, which leads to distortions compared to the gas-phase structure).

The calculated total energies and dipole moments of uracil, obtained with MP2 and a selection of different basis sets, are listed in Table 2, where they are compared to results from previous studies. We have also included the dipole moments computed with DZPi and ESP (i.e., the ESPB basis set without the bond functions) at the aug-cc-pVDZ geometry, since these

TABLE 2: Calculated Energies and Dipole Moments of Uracil

method	ref	basis set	total energy in E_h	dipole moment ^a in Debye
MP2	this work	6-311G*	–413.800 398	4.12
MP2	this work	6-31+G* ^b	–413.661 689	4.59
MP2	this work	aug-cc-pVDZ	–413.779 025	4.37
MP2	this work	DZPi	–413.457 228	4.29
MP2	this work	DZPi ^c	–413.451 720	4.20
MP2	this work	ESP ^c	–413.461 176	4.23
MP2	39	DZ		4.85
MP2	39	DZ+d ^d		4.43
MP2	38	[5s3p2d][3s2p]		4.35
exptl ^e	33			3.87 ± 0.4

^a Computed using Cartesian basis functions. ^b This basis set uses six-component d functions. ^c Computed at aug-cc-pVDZ-optimized geometry. ^d Exponents of d-polarization functions optimized to minimize dipole moment of imidazole. ^e Derived from microwave spectrum.

TABLE 3: MP2 Interaction Energies of the Global Minimum of Uracil–Water for Selected Basis Sets (All Energies in kJ/mol)

basis	no. basis functions	optimi- zation	D_e (no CP)	D_e (CP)	ΔU^{def} uracil	ΔU^{def} water
6-311G*	180	full	–59.27	–39.25	1.55	0.36
6-31+G*	183	full	–52.85	–41.60	1.12	0.48
DZPi	165	full	–64.17	–42.71	2.69	1.34
DZPi	165	frozen ^a	–61.04	–41.44	0.00	0.00
DZPi	165	frozen ^b	–57.77	–38.88	0.00	0.00
ESPB	182	no ^c	–97.60	–40.03	0.00	0.00
Rybak et al. ^d	geometry A			–43.4		
	geometry B			–44.4		

^a Uracil and H₂O monomers frozen at DZPi-optimized geometry. ^b Uracil frozen at aug-cc-pVDZ geometry, H₂O frozen at 6-311++G-(2d,2p) geometry. ^c Single-point calculation at DZPi-optimized geometry (with uracil and water monomers fixed at aug-cc-pVDZ and 6-311++G(2d,2p) geometry, respectively). ^d Reference 11. Results obtained from SAPT calculations with a minimal basis plus polarization function basis set. Geometry A from no-CP SCF/DZPi calculations. Geometry B from minimal basis no-CP SCF calculations.

geometry/basis set combinations are used to compute the interaction energy in the next sections. All computed dipole moments are somewhat larger than the experimental (gas-phase) value obtained from the microwave spectrum of uracil.³² However, the dipole moments computed with DZPi fall within the (large) error bars of the experimental result. We would like to note that the dipole moments in Table 1 are obtained with different methods (in this work, the dipole moments were obtained analytically from the linear response density matrix, while Johnson et al.³⁹ and Basch et al.⁴⁰ used numerical methods), which may lead to slightly different results.

Figure 2 shows the direction of the uracil dipole moment. The general direction is a little basis-set-dependent. As expected, the dipole moment points away from the side with the two (negatively charged) C=O groups.

3.2. Interaction Energy and Structure of the Global Uracil–Water Minimum. Table 3 lists the interaction energy D_e of the global minimum of the uracil–water complex (structure 1 in Figure 1), calculated with MP2 and several selected basis sets.

Comparison of the first three rows in Table 3 reveals the good performance of the relatively compact DZPi basis set. Although DZPi is smaller than either 6-31+G* or 6-311G*, it recovers a larger part of the interaction energy, likely because the DZPi basis set is specifically designed for the computation of interaction energies.

The deformation energy is small at the optimized minimum (see Table 3), indicating that the monomer geometries change little upon complex formation. The uracil interatomic bond distances change by less than 0.01 Å except those involved in forming the hydrogen bonds, i.e., the CO and NH bonds, which are elongated by about 0.02 Å. Similarly, the water OH bond that is involved in hydrogen-bonding is elongated by 0.02 Å, while the other OH bond changes by only 0.001 Å. This is consistent with the results of Broo and Holmén,⁴¹ who fully optimized the geometries of the cytosine–water complex. In the most stable cytosine–water conformer, which has a geometry very similar to the global uracil–water minimum, the CO and NH bonds are slightly elongated compared to the gas-phase cytosine, but otherwise, only minor changes occur upon complex formation. Similarly, Paglieri et al.⁴² studied solvent effects of uracil and cytosine using Onsager's reaction field model within the DFT framework and found that the uracil geometry shows very little change upon solvation.

This insignificant change in the monomer geometries upon complex formation results in a small change (less than 2 kJ/mol) in the interaction energy if the monomers are kept fixed at the DZPi-optimized geometries during the optimization. It therefore seems a reasonable approximation to restrict monomer relaxation during the optimization of the other points on the surface.

Thus, using the DZPi basis set, we performed uracil–water optimizations with the uracil and water monomers fixed at the more accurate aug-cc-pVDZ geometry and 6-311++G(2d,2p) geometries, respectively. At the optimized uracil–water geometry we subsequently performed a single-point calculation with the ESPB basis set, which increases the interaction energy by 1.1 kJ/mol. Note the huge increase in BSSE in this calculation, which is mainly due to the set of bond functions in ESPB. Clearly, basis sets such as ESPB can only be used for BSSE-corrected calculations.

The interaction energies reported in Table 3 are evaluated at the geometries optimized without application of the counterpoise procedure, and consequently, the geometrical parameters may be contaminated with BSSE. The error will be largest for geometries for which the intermolecular interaction is weak. To obtain an estimate of the effect of BSSE on the two hydrogen bond distances, we evaluated the counterpoise-corrected interaction energy, at the MP2/DZPi level of theory, at various values of $R(\text{O}\cdots\text{H}_w)$ and $R(\text{O}_w\cdots\text{H})$ (for further details on these calculations, see section 2.2). The initial $\text{O}\cdots\text{H}_w$ and $\text{O}_w\cdots\text{H}$ distances, obtained from the uncorrected optimizations, are 1.889 and 1.890 Å. The water monomer was first moved along the $\text{O}\cdots\text{H}_w$ direction, resulting in an optimum $\text{O}\cdots\text{H}_w$ distance of 2.007 Å. Moving the water parallel to $R(\text{O}\cdots\text{H}_w)$ unavoidably increases $R(\text{O}_w\cdots\text{H})$ as well; with $R(\text{O}\cdots\text{H}_w)$ equaling 2.007 Å, $R(\text{O}_w\cdots\text{H})$ is elongated to 1.966 Å. Starting with this geometry, we subsequently displaced the water parallel to the $\text{O}_w\cdots\text{H}$ bond. The resulting $\text{O}\cdots\text{H}_w$ and $\text{O}_w\cdots\text{H}$ distances are 2.03 and 2.00 Å, respectively, i.e., about 0.1 Å longer than the corresponding values obtained from the uncorrected optimization. This is in agreement with the difference between the counterpoise-corrected and uncorrected hydrogen bond distance in the water dimer.²² With MP2 and an ESP (extended s set augmented with one set of polarization functions) basis set an uncorrected optimization gives a hydrogen bond distance shorter by 0.14 Å than the corresponding value from counterpoise-corrected calculations. The $(\text{H}_2\text{O})_2$ interaction energy at the CP-corrected intermolecular distance is as much as 6.4 kJ/mol more negative than the interaction energy at the uncorrected geometry.

The uracil–water interaction energy seems to be less sensitive to minor changes in the hydrogen-bond distances; at the reoptimized geometry the interaction energy is only 1.4 kJ/mol more negative than the interaction energy at the no-CP optimized geometry.

Although the above procedure does not take into account any BSSE effects on the computed angles or dihedral angles, or any codependence of the geometrical parameters, we expect that further optimization will affect the hydrogen bond distances by less than 0.05 Å and the interaction energy by less than 1 kJ/mol.

Since no experimental value for the uracil–water interaction energy has been reported so far, we can only compare our results to an experimental result on a closely related compound. Sukhodub⁴³ presented the water association enthalpies of alkyl derivatives of nucleic acid bases in a vacuum, obtained using temperature-dependent field ionization mass spectrometry (TD-FIMS). The enthalpy of the monohydrate of 1-methyluracil was measured to be -46.9 kJ/mol, which is slightly larger than the interaction energy we obtain for uracil–water.

The only theoretical calculation of the uracil–water interaction energy including the dispersion energy and other correlation effects was done by Rybak et al.,¹¹ using SAPT (symmetry-adapted perturbation theory) and a minimal basis set augmented with one polarization function on all atoms. Their calculations were performed at two planar geometries. In one of these the monomer geometries were taken from crystallographic data, which may not be the optimal choice for gas-phase calculations. The other configuration uses monomer geometries obtained from SCF calculations. The uracil intramolecular bond lengths in this configuration differ from those optimized with MP2/aug-cc-pVDZ by 0.01–0.05 Å, while the intramolecular angles differ by up to 10°. The intermolecular parameters listed in ref 11, which are obtained from no-CP SCF calculations, are also quite different from those optimized in the present study. First of all, the two configurations used by Rybak et al. are planar, while our optimizations showed that one of the water hydrogen atoms points out of the plane of the uracil molecule. The $\text{O}_w\text{H}_w\cdots\text{O}$ hydrogen bond angle in one of the configurations considered by Rybak et al. (151.2°) agrees well with our result of 149.1°, but the intermolecular $\text{O}\cdots\text{O}$ distance (3.10 Å) is much longer than our optimized value of 2.75 Å. Despite the significant differences in geometry, the SAPT results (-43.4 and -44.4 kJ/mol) are in fairly good agreement with our computed D_e .

3.3. Interaction Energies and Structures of the Four Uracil–Water Minima. Table 4 lists the interaction energies and intermolecular structural parameters of the four minima investigated in this work, obtained from MP2 optimizations with the DZPi basis set, in which the uracil and water geometries are frozen at the aug-cc-pVDZ and 6-311++G(2d,2p) optimized geometries, respectively. For all minima, we additionally performed a single-point calculation with the ESPB basis set at the DZPi-optimized geometry, which increases the interaction energy by about 1 kJ/mol for all four minima.

Structure **1** is the most stable uracil–water minimum. Structures **2** and **3** are very close in energy, and within 10 kJ/mol of the global minimum. As expected, structure **4** is less stable than the other minima, since it contains only one strong hydrogen bond. The order of stability of the four structures is consistent with the results of Smets et al.¹² They found that structure **1** is the most stable complex, with **3** and **2** less stable by 6.5 and 7.9 kcal/mol, while we find energy differences of 6.6 and 8.2 kJ/mol. Note though that because Smets et al. did not compute interaction energies (they only reported total

TABLE 4: Interaction Energy (in kJ/mol) and Intermolecular Geometry (Distances in Å, Angles in deg) of the Four Uracil–Water Minima Obtained from Frozen-Monomer Calculations with MP2 and the DZPi Basis Set

property	basis set	structure 1	structure 2	structure 3	structure 4
Interaction Energies					
D_e (CP)	DZPi	-38.88	-30.80	-32.41	-25.33
D_e (CP)	ESPB ^a	-40.03	-31.83	-33.46	-26.61
Intermolecular Geometrical Parameters ^b					
$R(\text{O}\cdots\text{H}_w)$		1.889	1.897	1.874	1.865
$R(\text{O}_w\cdots\text{H})$		1.890	1.950	1.929	2.219
$\angle(\text{O}_w\text{H}_w\cdots\text{O})$		149.1	149.9	150.9	159.8
$\angle(\text{NH}\cdots\text{O}_w)^c$		143.4	141.7	142.4	129.7
$\text{HOH}\cdots\text{O}$		222.9	230.3	130.3	179.5

^a Single-point calculation at DZPi-optimized geometry with uracil and water monomers fixed at aug-cc-pVDZ and 6-311++G(2d,2p) geometry, respectively. ^b The w subscript indicates the atom belongs to the water moiety. ^c $\text{CH}\cdots\text{O}_w$ for structure 4.

uracil–water energies), their results are not corrected for BSSE. We find that the BSSE is large (16–19 kJ/mol) in all four minima. Despite this, however, BSSE appears not to change the order of stability of the minima.

The water molecule is arranged in such a way to allow the intermolecular bonds to assume a cyclic structure, with the water OH bond that is involved in the cyclic arrangement situated in the plane of the uracil molecule. In structures 1–3, the $\text{O}\cdots\text{H}_w$ and $\text{O}_w\cdots\text{H}$ distances are of comparable size. Similarly, the $\text{O}_w\text{H}_w\cdots\text{O}$ and $\text{NH}\cdots\text{O}_w$ hydrogen bond angles are of comparable magnitude. The $\text{O}_w\text{H}_w\cdots\text{O}$ angle is around 150°, while the $\text{NH}\cdots\text{O}_w$ angle is a bit smaller (about 140°). These angles are significantly nonlinear. It is well-recognized that the optimum hydrogen bond angles are largely determined by the electrostatic contribution to the interaction energy,⁴⁴ and an (oversimplified) electrostatic model, with the electrostatic interaction as the interaction between a polar XH group and a partially negative Y-atom, would result in a clear preference for linear $\text{X}-\text{H}\cdots\text{Y}$ hydrogen bonds, particularly if the XH bond is very polar. Other contributions to the interaction energy (like electrostatic terms arising from higher-than-dipole multipole moments and exchange–repulsion contributions) may, however, favor nonlinear hydrogen bond geometries (resulting in strongly nonlinear geometries in, for example, the water–formaldehyde complex,⁴⁵ in which the $\text{OH}\cdots\text{O}$ deviates from linearity by as much as 30°). Kroon et al.⁴⁶ have shown that a large majority of $\text{OH}\cdots\text{O}$ hydrogen bonds found in crystal structures are nonlinear by at least 10°, in many cases because of an energetical preference for nonlinearity. Likewise, Lommerse et al.⁴⁷ found that slightly bent hydrogen bonds are often a bit more favorable, owing to an enhanced interaction between the donor and acceptor molecule. In the present case, the nonlinear hydrogen bond angles are probably mainly the result of the increased stability arising from the formation of two hydrogen bonds.

Whereas there is no distinct preference for hydrogen bond formation along the lone-pair directions for water and ether (sp^3) type oxygen atoms,^{46,47} for carbonyl (sp^2) oxygens a lone-pair preference does seem to exist.⁴⁷ Apaya et al.,⁴⁸ however, have shown for formaldehyde that the electrostatic potential around the carbonyl oxygen is very flat, and as a result, other interactions may have a large effect on the structure of the $\text{OH}\cdots\text{O}(=\text{C})$ hydrogen bond. Likewise, for complexes containing $\text{NH}\cdots\text{O}(=\text{C})$ hydrogen bonds it has been found⁴⁹ that the observed preference for bonding in the lone-pair direction mainly arises from geometrical constraints involved in maximiz-

TABLE 5: Interaction Energy (in kJ/mol) and Intermolecular Geometry (Distances in Å, Angles in deg) of the Transition State between Minima 1 and 2

basis set	D_e (CP)	$R(\text{O}\cdots\text{H}_w)$	$\angle(\text{O}_w\text{H}_w\cdots\text{O})$	$\text{H}_w\cdots\text{OCN}$
DZPi ^a	-17.10	1.869	158.5	80.6
DZPi ^b	-16.71	1.877	160.4	80.2
DZPi ^c	-15.96	1.906	156.3	79.1
ESPB ^d	-17.11			

^a Full optimization. ^b Uracil and H_2O monomers frozen at DZPi-optimized geometry. ^c Uracil frozen at aug-cc-pVDZ geometry, H_2O frozen at 6-311++G(2d,2p) geometry. ^d Single-point calculation at DZPi-optimized geometry (with uracil and water monomers fixed at aug-cc-pVDZ and 6-311++G(2d,2p) geometry, respectively).

ing the number of favorable intermolecular interactions. In all four uracil–water minima the hydrogen-bonding H_w atom roughly points toward one of the lone pairs of the uracil carbonyl atom, but this rearrangement is likely not so much the result of lone-pair directionality but rather of the formation of the second ($\text{NH}\cdots\text{O}$ or $\text{CH}\cdots\text{O}$) hydrogen bond.

The water H-atom that is not involved in the cyclic hydrogen-bonded arrangement is pointing out of the plane in geometries 1–3, as quantified by the dihedral angle listed in the last row of Table 4. This arrangement brings the water lone-pair region, which lies perpendicular to the $\text{H}_w\text{O}_w\text{H}_w$ plane, toward the uracil plane. There is a greater flexibility within (or parallel to) the plane of the water lone pairs,^{46,50} and it has been shown⁴⁷ that the electrostatic contribution to the interaction energy strongly favors a position in the plane of the lone pairs of ether and carbonyl groups for the hydrogen-bonding H-atom. Optimizations of uracil–water with ORIENT,² using a model potential consisting of a hard-sphere repulsion and an electrostatic contribution, yielded nonflat structures for all four minima, with the water hydrogen sticking out of the plane of the uracil molecule. The electrostatic interaction energy was calculated from a distributed multipole (DMA) model, and since the only other term in the model potential was a hard-sphere repulsion, the preference for the hydrogen to be out-of-plane must be due to the electrostatic contribution.

The weakly bound minimum 4, which has a $\text{CH}\cdots\text{O}_w$ and $\text{O}_w\text{H}_w\cdots\text{O}(=\text{C})$ hydrogen bond, has the water coplanar with the uracil molecule (the $\text{H}_w\text{O}_w\text{H}_w\cdots\text{O}$ dihedral angle is nearly 180°; see Table 4). However, the potential appears to be very flat for the non-hydrogen-bonded water proton to rotate out of the plane. Optimizations with MP2 and the 6-31G* basis set produced a noncoplanar structure ($\text{H}_w\text{O}_w\text{H}_w\cdots\text{O}$ dihedral angle is 94°), as did the electrostatic + hard-sphere model. Evidently, the electrostatic-driven preference for hydrogen bonding in the lone-pair plane of the water oxygen seems very weak for the $\text{C}-\text{H}\cdots\text{O}$ interaction.

The $\text{O}_w\cdots\text{H}(-\text{C})$ hydrogen bond distance is 0.35 Å longer than the $\text{O}\cdots\text{H}_w$ bond in minimum 4. This is consistent with the larger $\text{X}\cdots\text{O}_w$ distance (X is C or O) found in methane–water compared to the water dimer.²⁰ $\text{CH}\cdots\text{O}$ hydrogen bonds are much weaker than $\text{OH}\cdots\text{O}$ and $\text{NH}\cdots\text{O}$ bonds, mainly because of a large reduction in the electrostatic contribution (since CH is much less polar than OH). The $\text{O}_w\text{H}_w\cdots\text{O}$ hydrogen bond angle in structure 4 is 160°, i.e., more linear, while the $\text{CH}\cdots\text{O}_w$ bond angle is with its 130° further from linearity than the corresponding angles in the other minimum-energy structures, also reflecting the weaker nature of the $\text{CH}\cdots\text{O}$ bond.

3.4. Interaction Energies and Structures of the Transition States. Table 5 lists the interaction energy and intermolecular geometrical parameters of the transition state determined between minimum 1 and minimum 2, which is shown in Figure

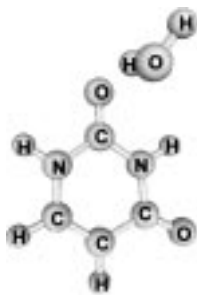


Figure 3. Optimized geometry of the transition state between minimum **1** and **2**. This structure contains only one (OH \cdots O) hydrogen bond. The water molecule is entirely above the plane of uracil.

TABLE 6: Interaction Energy (in kJ/mol) and Intermolecular Geometry (Distances in Å, Angles in deg) of the Transition State between Minima 2 and 3

basis set	D_c (CP)	$R(\text{O}_w\cdots\text{H})$	$\angle(\text{NH}\cdots\text{O}_w)$	$\angle(\text{H}_w\text{O}_w\cdots\text{H})$
DZPi ^a	-24.59	1.77	177.3	108.5
DZPi ^b	-23.86	1.80	177.5	109.4
DZPi ^c	-22.61	1.81	178.0	112.7
ESPB ^d	-23.26			

^a Full optimization. ^b Uracil and H₂O monomers frozen at DZPi-optimized geometry. ^c Uracil frozen at aug-cc-pVDZ geometry, H₂O frozen at 6-311++G(2d,2p) geometry. ^d Single-point calculation at DZPi-optimized geometry (with monomers fixed at the aug-cc-pVDZ and 6-311++G(2d,2p) geometry.

3. The transition state contains only one hydrogen bond. The NH \cdots O hydrogen bond occurring in the two neighboring minimum-energy structures has been broken, and the water OH bond involved in forming the cyclic hydrogen-bonded arrangement in structures **1** and **2** has moved out of plane. This is apparent from the H_w \cdots OCN (and O_w \cdots OCN) dihedral angle listed in the last column of Table 5, which indicates the position of the water hydrogen-bonding H_w (or O_w) atom with respect to the plane of the uracil molecule. This angle equals approximately (within a few degrees) 180° and 0° in minima **1** and **2**, respectively, denoting that the H_w and O_w atoms are in the uracil plane in these structures, while it is 79° (80°) in the transition-state structure. The O_w \cdots H hydrogen bond distance is 1.91 Å, i.e., slightly longer than the corresponding distance in structures **1** and **2**. The O_wH_w \cdots O hydrogen bond angle is 156°, which is larger (i.e., more linear) than in structures **1** and **2**.

The transition state is estimated to be 22.9 kJ/mol higher in energy than minimum **1** and 14.7 kJ/mol higher in energy than minimum **2**. It therefore seems unlikely that zero-point vibrational motion will be sufficient to overcome this barrier, and we expect that water molecules in their zero-point motion do not exhibit substantial movement between the global minimum and the other hydration sites in uracil–water clusters.

Table 6 lists the interaction energy and intermolecular geometrical parameters of the transition state connecting minimum **2** and minimum **3**. The optimized geometry is shown in Figure 4. The water oxygen atom is in the plane of the uracil molecule, while the two water hydrogens point out of the plane. Minima **2** and **3** are almost equally stable, and the transition state is located symmetrically between them. The two O_wH_w \cdots O angles are identical within tenths of a degree, and the NH \cdots O_w angle is approximately linear (see Table 6). Movement of a water molecule from structure **2** to structure **3** and vice versa involves a simple O_wH_w \cdots O hydrogen bond exchange, and the transition-state structure therefore contains only one (NH \cdots O_w) hydrogen bond. This hydrogen bond is shorter than the corresponding NH \cdots O_w bond in minima **2** and **3**. With ESPB,

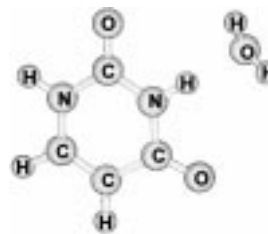


Figure 4. Optimized geometry of the transition state between minima **2** and **3**, containing an approximately linear (NH \cdots O) hydrogen bond. The water oxygen atom is in the plane of the uracil molecule, while the two water hydrogens point out of the plane.

the interaction energy of this transition-state structure is -23.3 kJ/mol, only 8.6 kJ/mol above structure **2** and 10.2 kJ/mol above structure **3**. In contrast to the transition state between minima **1** and **2**, the water oxygen atom remains in the uracil plane, and the only atoms that have to move out of the plane are light hydrogen atoms. We intend to establish if zero-point vibrational motion is sufficient to overcome this barrier, which is not much higher than the zero-point energy computed in preliminary DMC calculations, employing simple potential models.⁵¹ This result may, however, change with more elaborate model potentials, and moreover, the effect of zero-point vibration on the barrier heights also needs to be taken into account.

The monomer geometries change little upon complex formation in both transition-state structures, consistent with the results for the global minimum. Full optimization of the complex geometry with DZPi shortens the two CN bonds closest to the water moiety by about 0.01 Å, while the distances involved in forming the hydrogen bond (i.e., the uracil CO and water OH bonds in the first transition state and the NH bond in the second transition state) are elongated by a similar amount. All other intermolecular distances change by at most 0.001 Å. Likewise, the change in interaction energy is less than 1 kJ/mol.

4. Summary

Owing to the size of the uracil molecule, accurate calculations on uracil–water present novel challenges, which cannot simply be overcome by enlarging the basis set.

The computationally desirable approximation of freezing the intramolecular geometries of the monomers was found to be small (less than 2 kJ/mol for the global minimum), indicating that in simulation studies not much accuracy is lost by treating the individual fragments as rigid bodies.

To correct for BSSE, the computation of the interaction energy at the optimized geometries was carried out using the counterpoise procedure. However, BSSE may also lead to errors in the optimized structure. This effect is often ignored because of the large amount of computation time needed for the corrections. In the present study we have investigated in an approximate way the effect of BSSE on the computed hydrogen bond distances of the global minimum, in an attempt to estimate the errors introduced by neglecting the effect of BSSE on the computed geometries. This effect was also found to be small for both the computed geometry and interaction energy. BSSE decreases the bond distances by about 0.1 Å, while the interaction energy at the geometry with the reoptimized hydrogen bond distances is increased by 1.4 kJ/mol.

In the current study we have located four minima, as well as two transition states, on the uracil–water potential energy surface using MP2 and the interaction-optimized DZPi basis set. Our best computed interaction energies for the four uracil–water minima are -40.0, -31.8, -33.5, and -26.6 kJ/mol. In

all four minima investigated in this work the water molecule is bound to the uracil moiety via two hydrogen bonds. The three most stable structures contain one $O_wH_w\cdots O$ and one $NH\cdots O_w$ hydrogen bond, which are of comparable length. The water oxygen and hydrogen atoms that are involved in forming the hydrogen bonds are in the plane of uracil, while the free water hydrogen atom points out of the plane. The fourth and least stable structure contains an $O_wH_w\cdots O$ and a considerably longer $CH\cdots O_w$ hydrogen bond. In this structure, there seems to be no clear preference for the water hydrogen that is not involved in forming the hydrogen bonds to be in or out of the plane of the uracil molecule.

The barrier height between structures **1** and **2** is as much as 23 kJ/mol, and it therefore seems unlikely that zero-point vibrational motion will cause substantial movement of single water molecules between the global minimum and the other hydration sites in uracil–water clusters. The barrier height between structures **2** and **3**, however, is substantially less (10 kJ/mol). Further study will be necessary to establish if vibrational zero-point motion will be sufficient to overcome the barrier between the local minima. The results presented in this paper will be used to improve existing model potentials for the uracil–water interaction, with the intent to simulate clusters of uracil surrounded by several waters molecules.

Acknowledgment. This work is supported by a grant from The Leverhulme Trust. We thank Dr. H. Früchtl for useful discussions and help with the NWChem program. We also gratefully acknowledge support from the Engineering and Physical Sciences Research Council.

References and Notes

- (1) Mok, D. K. W.; Handy, N. C.; Amos, R. D. *Mol. Phys.* **1997**, *92*, 667.
- (2) Stone, A. J. *ORIENT*, version 3.2g (with contributions from Dullweber, A.; Hodges, M. P.; Popelier, P. L. A.; Wales, D. J.); University of Cambridge, 1996.
- (3) Stone, A. J. *Chem. Phys. Lett.* **1981**, *83*, 233.
- (4) Stone, A. J.; Alderton, M. *Mol. Phys.* **1985**, *56*, 1047.
- (5) Buckingham, A. D.; Fowler, P. W.; Stone, A. J. *Int. Rev. Phys. Chem.* **1986**, *5*, 107.
- (6) Gregory, J. K.; Clary, D. C. *Chem. Phys. Lett.* **1995**, *237*, 39.
- (7) Brown, D. F. R.; Gregory, J. K.; Clary, D. C. *J. Chem. Soc., Faraday Trans.* **1996**, *92*, 11.
- (8) Gregory, J. K.; Clary, D. C. *J. Chem. Phys.* **1996**, *105*, 6626.
- (9) Gregory, J. K.; Clary, D. C. *J. Phys. Chem.* **1996**, *100*, 18014.
- (10) Sorenson, J. M.; Gregory, J. K.; Clary, D. C. *J. Chem. Phys.* **1997**, *106*, 849.
- (11) Rybak, S.; Szalewicz, K.; Jeziorski, B.; Corongiu, G. *Chem. Phys. Lett.* **1992**, *199*, 567.
- (12) Smets, J.; McCarthy, W. J.; Adamowicz, L. *J. Phys. Chem.* **1996**, *100*, 14655.
- (13) Smets, J.; Smith, D. M. A.; Elkadi, Y.; Adamowicz, L. *J. Phys. Chem. A* **1997**, *101*, 9152.
- (14) Sagarik, K.; Corongiu, G.; Clementi, E. *THEOCHEM* **1991**, *81*, 355.
- (15) Del Bene, J. E. *J. Comput. Chem.* **1981**, *2*, 188.
- (16) van Duijneveldt, F. B.; van Duijneveldt-van de Rijdt, J. G. C. M.; van Lenthe, J. H. *Chem. Rev.* **1994**, *94*, 1873.
- (17) van Mourik, T.; Wilson, A. K.; Peterson, K. A.; Woon, D. E.; Dunning, T. H., Jr. *Adv. Quantum Chem.* **1999**, *31*, 105.
- (18) Peterson, K. A.; Dunning, T. H., Jr. *J. Chem. Phys.* **1995**, *102*, 2032.
- (19) Xantheas, S. S. *J. Chem. Phys.* **1996**, *104*, 8821.
- (20) van Duijneveldt-van de Rijdt, J. G. C. M.; van Duijneveldt, F. B. In *Theoretical Treatments of Hydrogen Bonding*; Hadži, D., Ed.; John Wiley & Sons Ltd.: New York, 1997.
- (21) Frisch, M. J.; Trucks, G. W.; Schlegel, H. B.; Gill, P. M. W.; Johnson, B. G.; Robb, M. A.; Cheeseman, J. R.; Keith, T.; Petersson, G. A.; Montgomery, J. A.; Raghavachari, K.; Al-Laham, M. A.; Zakrzewski, V. G.; Ortiz, J. V.; Foresman, J. B.; Cioslowski, J.; Stefanov, B. B.; Nanayakkara, A.; Challacombe, M.; Peng, C. Y.; Ayala, P. Y.; Chen, W.; Wong, M. W.; Andres, J. L.; Replogle, E. S.; Gomperts, R.; Martin, R. L.; Fox, D. J.; Binkley, J. S.; Defrees, D. J.; Baker, J.; Stewart, J. P.; Head-Gordon, M.; Gonzalez, C.; Pople, J. A. *Gaussian 94*, revision E.1; Gaussian, Inc.: Pittsburgh, PA, 1995.
- (22) van Duijneveldt-van de Rijdt, J. G. C. M.; van Duijneveldt, F. B. *J. Chem. Phys.* **1992**, *97*, 5019.
- (23) van Mourik, T. Ph.D. Thesis, University Utrecht, 1994.
- (24) Dunning, T. H., Jr. *J. Chem. Phys.* **1970**, *53*, 2823.
- (25) Dunning, T. H., Jr.; Hay, P. J. In *Methods of Electronic Structure Theory*; Schaefer, H. F., III, Ed.; Plenum Press: New York, 1977; Vol. 2.
- (26) van Lenthe, J. H.; van Duijneveldt, F. B. *J. Chem. Phys.* **1984**, *81*, 3168.
- (27) Dunning, T. H., Jr. *J. Chem. Phys.* **1989**, *90*, 1007.
- (28) Krishnan, R.; Binkley, J. S.; Seeger, R.; Pople, J. A. *J. Chem. Phys.* **1980**, *72*, 650.
- (29) Hariharan, P. C.; Pople, J. A. *Theor. Chim. Acta* **1973**, *28*, 213.
- (30) Clark, T.; Chandrasekhar, J.; Spitznagel, G. W.; Schleyer, P. v. R. *J. Comput. Chem.* **1983**, *4*, 294.
- (31) Gill, P. M. W.; Johnson, B. G.; Pople, J. A.; Frisch, M. J. *Chem. Phys. Lett.* **1992**, *197*, 499.
- (32) Brown, R. D.; Godfrey, P. D.; McNaughton, D.; Pierlot, A. P. *J. Am. Chem. Soc.* **1988**, *110*, 2329.
- (33) Boys, S. F.; Bernardi, F. *Mol. Phys.* **1970**, *19*, 553.
- (34) Frisch, M. J.; Del Bene, J. E.; Binkley, J. S.; Schaefer, H. F., III. *J. Chem. Phys.* **1986**, *84*, 2279.
- (35) MOLPRO96 is a suite of ab initio programs written by Werner, H.-J. Knowles, P. J., with contributions by Almlöf, J.; Amos, R. D.; Deegan, M. J.; Elbert, S. T.; Hampel, C.; Meyer, W.; Peterson, K. A.; Pitzer, R. M.; Reinsch, E.-A.; Stone, A. J.; Taylor, P. R.
- (36) Anchell, J.; Apra, E.; Bernholdt, D.; Borowski, P.; Clark, T.; Clerc, D.; Dachsels, H.; Deegan, M.; Dupuis, M.; Dyall, K.; Fann, G.; Früchtl, H.; Gutowski, M.; Harrison, R.; Hess, A.; Jaffe, J.; Kendall, R.; Kobayashi, R.; Kutteh, R.; Lin, Z.; Littlefield, R.; Long, X.; Meng, B.; Nichols, J.; Nieplocha, J.; Rendall, A.; Stave, M.; Straatsma, T.; Taylor, H.; Thomas, G.; Wolinski, K.; Wong, A. *NWChem, A Computational Chemistry Package for Parallel Computers*, version 3.1; Pacific Northwest National Laboratory: Richland, WA, , 1997.
- (37) Frisch, M. J.; Head-Gordon, M.; Pople, J. A. *Chem. Phys. Lett.* **1990**, *166*, 275.
- (38) Stewart, R. F.; Jensen, L. H. *Acta Crystallogr.* **1967**, *23*, 1102.
- (39) Johnson, R. C.; Power, T. D.; Holt, J. S.; Immaraporn, B.; Monat, J. E.; Sissoko, A. A.; Yanik, M. M.; Zagardny, A. V.; Cybulski, S. M. *J. Phys. Chem.* **1996**, *100*, 18875.
- (40) Basch, H.; Garmer, D. R.; Jasien, P. G.; Krauss, M.; Stevens, W. *J. Chem. Phys. Lett.* **1989**, *163*, 514.
- (41) Broo, A.; Holmén, A. *J. Phys. Chem. A* **1997**, *101*, 3589.
- (42) Paglieri, L.; Corongiu, G.; Estrin, D. A. *Int. J. Quantum Chem.* **1995**, *56*, 615.
- (43) Sukhodub, L. F. *Chem. Rev.* **1987**, *87*, 589.
- (44) Bonaccorsi, R.; Petrongolo, C.; Scrocco, E.; Tomasi, J. *Theor. Chim. Acta* **1971**, *20*, 331.
- (45) Vos, R. J.; Hendriks, R.; van Duijneveldt, F. B. *J. Comput. Chem.* **1990**, *11*, 1.
- (46) Kroon, J.; Kanters, J. A.; van Duijneveldt-van de Rijdt, J. G. C. M.; van Duijneveldt, F. B.; Vliegthart, J. A. *J. Mol. Struct.* **1975**, *24*, 109.
- (47) Lommerse, J. P. M.; Price, S. L.; Taylor, R. *J. Comput. Chem.* **1997**, *18*, 757.
- (48) Apaya, R. P.; Bondi, M.; Price, S. L. *J. Comput.-Aided Mol. Design* **1997**, *11*, 479.
- (49) Mitchell, J. B. O.; Price, S. L. *Chem. Phys. Lett.* **1989**, *154*, 267.
- (50) van Mourik, T.; van Duijneveldt, F. B. *THEOCHEM* **1995**, *341*, 63.
- (51) van Mourik, T.; Benoit, D. E.; Clary, D. C. Work in progress.
- (52) Aamouche, A.; Ghomi, M.; Coulombeau, C.; Jobic, H.; Grajcar, L.; Baron, M. H.; Baumruk, V.; Turpin, P. Y.; Henriët, C.; Berthier, G. *J. Phys. Chem.* **1996**, *100*, 5224.